Electronic Supplementary Material

Fabrication and high ORR performance of MnO$_x$ nanopyramid layers with enriched oxygen vacancies

Yong Zhang[a], Chengcheng Wang[a], Jiali Fu[a], Hui Zhao[a], Fang Tian[a] and Renjie Zhang[a,b,c]*

[a] Key Laboratory of Colloid and Interface Chemistry of the Ministry of Education of the P. R. China, Shandong University, Jinan 250100, P. R. China

[b] National Engineering Technology Research Center for Colloidal Materials, Shandong University, Jinan 250100, P. R. China

[c] Key Laboratory of Special Functional Aggregated Materials of the Ministry of Education of the P.R. China, Shandong University, Jinan 250100, P. R. China.

*Corresponding author, Email: zhrj@sdu.edu.cn

EXPERIMENTAL

1. Materials

Octadecyltrichlorosilane (OTS), 2,2,4-trimethylpentane, Nafion perfluorinated resin solution (5 wt% in mixture of lower aliphatic alcohols and water, contains 45 wt% water) were purchased from Sigma-Aldrich Co., LLC. Copper sulfate (CuSO$_4$), potassium permanganate (KMnO$_4$), potassium hydroxide (KOH), and ethanol were purchased from Sinopharm Chemical Reagents Co., Ltd. Polydimethylsiloxane (PDMS, SYLGARD 184 silicone elastomer base and agent) was purchased from Dow Corning Corporation. Water-soluble chitosan (CS, Mw = 50000 g mol^{-1}) was purchased from Jinan Haidebei Marine Bioengineering Co. Ltd. Commercial Pt/C (20 wt% Pt) was from Aladdin Co., Ltd. Al$_2$O$_3$ powder of 0.3 μm in diameter was purchased from Wuhan GaossUnion Co., Ltd. They were all analytical grade reagents and directly used without further purification. Pure water with a resistivity of 18.2 MΩ cm^{-1} at 25 ºC was used in all experiments.

2. Experimental Section

2.1 Fabrication of PDMS mold

2,2,4-trimethylpentane (15.0 mL) was added into a beaker (5.0 mL). Then, CuSO$_4$ powders were added in the beaker for removing water in solution. Then the solution,

Octadecyltrichlorosilane (OTS) and a syringe filter were first put into a glove bag, which was removed air under vacuum (10 KPa, 5 min) followed by filling pure N_2 to avoid moisture. A syringe filter (0.22 μm pore diameter) was used to remove $CuSO_4$ in the solution. Then OTS (1.5 g) was added into the solution and homogenously mixed. A home-made polypropylene (PP) block (46 mm × 27 mm × 10 mm) for later PDMS cell was etched by oxygen plasma for 1 min for each surface. Then, the PP block was immersed into OTS solution in 2,2,4-trimethylpentane for 3 min, followed by washing unadsorbed OTS molecule using dehydrated 2,2,4-trimethylpentane by $CuSO_4$. A square Teflon cell with the inner dimension of 60 mm × 35 mm × 20 mm was used to prepare PDMS mold. The precursors of PDMS base (20.0 g) and PDMS agent (2.0 g) were mixed and continuously stirred for 30 min at room temperature. A part of the precursor mix was added into square Teflon cell, then the PP block was very slightly put on the surface of PMDS mix in the Teflon cell. The left PDMS was slightly added into the interval between the Teflon cell and PP block. The cell was then degassed under vacuum (10 KPa, 30 min) for 5 times to remove air bubbles in PDMS, followed by polymerization at 70 °C for 2 h. After cooling down to the room temperature, the PMDS mold with the inner dimension of 46 mm × 27 mm × 7 mm was obtained by peeling off the Teflon cell and PP block.

2.2 Preparation of N doped carbon (NC) laminated arrays

Firstly, laminated CS arrays were prepared. Water-soluble CS with different mass ratio of 3, 4, 5 and 6 wt% were dispersed in 10.0 mL of water under vigorous stirring, respectively, followed by continually stirring for 10 h to be completely dissolved. Each CS solution was degassed by sonication and vacuumization, then poured into the PDMS mold placed on an end of a 90° folded steel plate. The other end of the steel plate was inserted into liquid nitrogen. Ice nucleus formed would grow along bidirection, inducing the formation of laminated ice and CS due to phase separation[1, 2]. After complete freezing, the samples were freeze dried to obtain laminated CS arrays, followed by annealing in a N_2 atmosphere (at a heating rate of 2 °C min^{-1} from room temperature to 500 °C and kept at 500 °C for 1 h, then 5 °C min^{-1} from 500 °C to 800 °C and kept at 800 °C for 2 h followed by cooling down to the room temperature). Thus,

NC laminated arrays were obtained.

2.3 Preparation of manganese oxide nanopyramids/NC (MONPMs/NC) laminated arrays

The laminated NC arrays (40 mg) were immersed into the $KMnO_4$ solution (25 mL, 0.4 mg mL^{-1}) under slightly stirring, followed by degassing under vacuum (10 KPa, 60 min) to remove air in the spacings of laminated NC. The mixture was then kept at 60 °C for 12 h. The obtained laminated MONPMs/NC arrays were rinsed by deionized water for four times followed rinsing with ethanol for one time, and finally dried at 60 °C for 4 h. MONPMs were obtained from MONPMs/NC after burning NC through annealing at 450 °C for 2 h under air atmosphere.

3. Characterization

Scanning electron microscopy (SEM) measurement was carried out on a Gemini300 (Zeiss, Germany) instrument under an operating voltage of 3 kV and an operating distance of 4 mm. The SEM species were prepared by cutting the samples using a knife, and then sputtered with gold. The elemental mapping was done on a high resolution energy dispersive X-ray spectrometer (Bruker, Germany) attached to the SEM. X-ray diffraction (XRD) patterns were collected by a D8 Advance X-ray diffractometer (Bruker, Germany) operated at 40 mA and 40 kV with the Cu (Kα) radiation (λ = 1.54184 Å) at a scanning rate of 4° min^{-1} and in an angular range of 8–80° at an interval of 0.02°. The instrumental line broadening was evaluated by measuring the XRD spectrum of annealing Si powder and the instrumental peak broadening was taken out by using the Jade software. X-ray photoelectron spectroscopy (XPS) was taken on a 250Xi spectrometer system (Thermo Scientific, USA) with the Al (Kα) radiation (X-ray energy 1486.6 eV) with an energy analyzer working in the pass energy mode at 100.0 eV. The binding energy was calibrated against the C1s line. The XPS samples were prepared by sticking 10 mg of NC or MONPMs/NC powders onto silicon substrates. Transmission electron microscopy (TEM) images were obtained by a JEM-1011 TEM (JEOL, Japan) with an acceleration voltage of 100 kV. High resolution TEM (HRTEM) images and selected area electron diffraction (SAED) were obtained on a JEOL-2100F TEM (JEOL, Japan) with an acceleration voltage of 200 kV. The TEM

species were prepared by dropping 5 μL of MONPMs/NC suspensions on copper grids followed by air drying. Raman spectra were obtained using the LabRAM HR 800 system (Horiba JY, France) excited with the laser of 633 nm. Nitrogen (N_2) adsorption-desorption isotherms were recorded with an ASAP 2020 HD88 instrument (Micromeritics, USA) at -197 °C. The specific surface area of MONPMs/NC was obtained by calculating the adsorption branch with BET method. The pore distributions of MONPMs/NC and MONPMs were obtained by automatically loading the installed program in the ASAP 2020 HD88, non-local density functional theory (NLDFT) with the international standard (ISO 15901-3:2007 - Part 3: Analysis of micropores by gas adsorption). Electron spin resonance (ESR) spectra were obtained with the JEOL JES-X320 at a frequency of 9.184 GHz at room temperature.

3. Electrochemical measurement

The LSV curves and chronoamperometric responses of MONPMs, NC, MONPMs/NC and commercial Pt/C (20 wt% Pt) were investigated on a CHI770C electrochemical work station (CHI770C, China) with a three-electrode system in an aqueous 0.1 M KOH. Glassy carbon rotating disk electrodes (RDE) of 5 mm in diameter separately modified by MONPMs, NC, MONPMs/NC and commercial Pt/C (20 wt% Pt) were used as working electrode. The Ag/AgCl (sat. KCl) and Pt foil were used as reference and counter electrodes, respectively. All the potentials values were calibrated with respect to the reversible hydrogen electrode (RHE) according to the equation: E (*vs.* RHE) =E (vs. Ag/AgCl) + 0.97 V in 0.1 M KOH. Before modification, the RDE was polished using Al_2O_3 powder and rinsed separately with water and ethanol for 3 times, respectively, then sonicated for 15 min, and dried by high purity N_2 stream. MONPMs/NC, MONPMs, and NC (2 mg) were purposely broken and separately dispersed in a mixture of ethanol (985 μL) and Nafion solution (15 μL). Subsequently, the above homogeneous suspensions (10 μL) were separately cast onto the surfaces of RDE and dried at room temperature. The loading amount of the active materials is 102 μg cm^{-2}. The working electrode was scanned at a rate of 5 mV s^{-1} with varying rotating speeds from 225 to 2500 rpm. Koueckýe-Levich (K-L) plots were analyzed at various electrode potentials. The slopes of their fitted linear lines were used to calculate average

electron transfer number (N) on the basis of the K-L equation:

$$\frac{1}{j} = \frac{1}{j_k} + \frac{1}{j_d} = \frac{1}{j_k} + \frac{1}{B \times \omega^{0.5}} = \frac{1}{j_k} + \frac{1}{B(2 \times \pi \times n)^{0.5}}$$

$$B = 0.2 \times N \times F \times v^{1/6} \times D^{2/3}C$$

where j is the measured current density (mA cm^{-2}), j_k and j_d are the kinetic- and diffusion-limiting current densities (mA cm^{-2}), ω is the angular velocity of the working electrode, n is the rotation speed of the working electrode (rpm), F is the Faraday constant (F=96485 C mol^{-1}), C is the bulk concentration of O_2 in 0.1 KOH (1.2×10^{-3} mol cm^{-3}), v is the kinematic viscosity of the electrolyte (0.01 cm^2 s^{-1}), and D is the diffusion coefficient of O_2 in 0.1 M KOH (1.9×10^{-5} cm^2 s^{-1}). For the Tafel plot, the kinetic current density measured at a rate of 5 mV s^{-1} with the rotating speed of 1600 rpm was calculated from the mass-transport correction of the RDE data by:

$$j_k = \frac{j \times j_d}{j_d - j}$$

The electrochemical impedance analysis was obtained by electrochemical impedance spectroscopy (EIS) using an impedance analyzer (Zahner IM6, Germany). The measurement was carried out in the frequency range of 0.1-10^5 Hz with voltage amplitude of 5 mV.
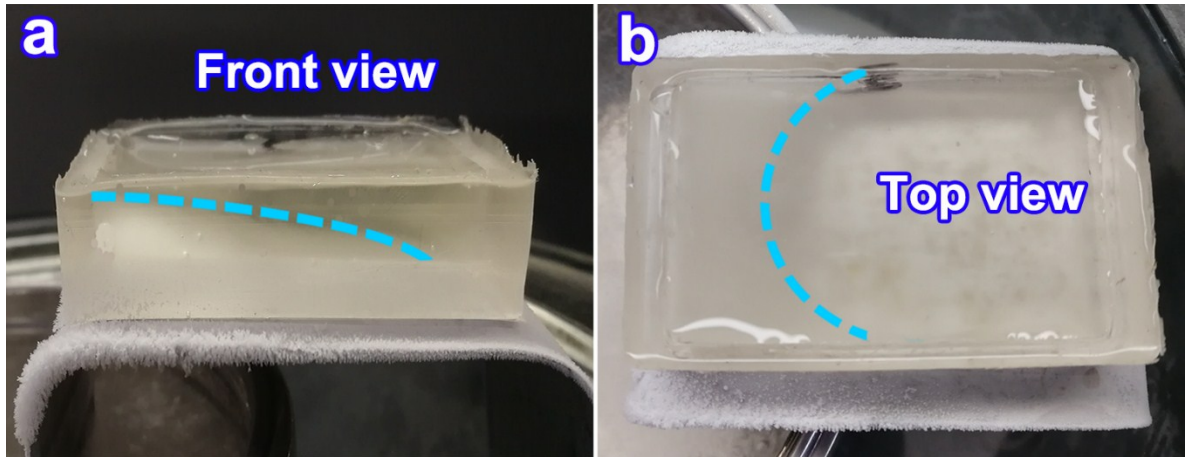
Fig. S1 a) Front view and b) top view of the 5 wt% CS solution in a PDMS mold on a steel plate after bidirectionally freezing for 15 min. The dotted lines illustrate the interface between solid and liquid.
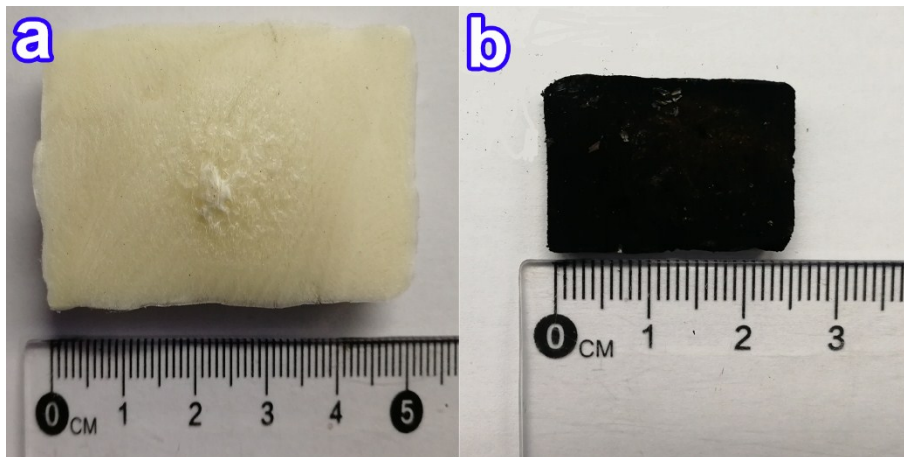
Fig. S2 Digital photographs of (a) laminated CS arrays and (b) laminated NC arrays after annealing at 800 °C.
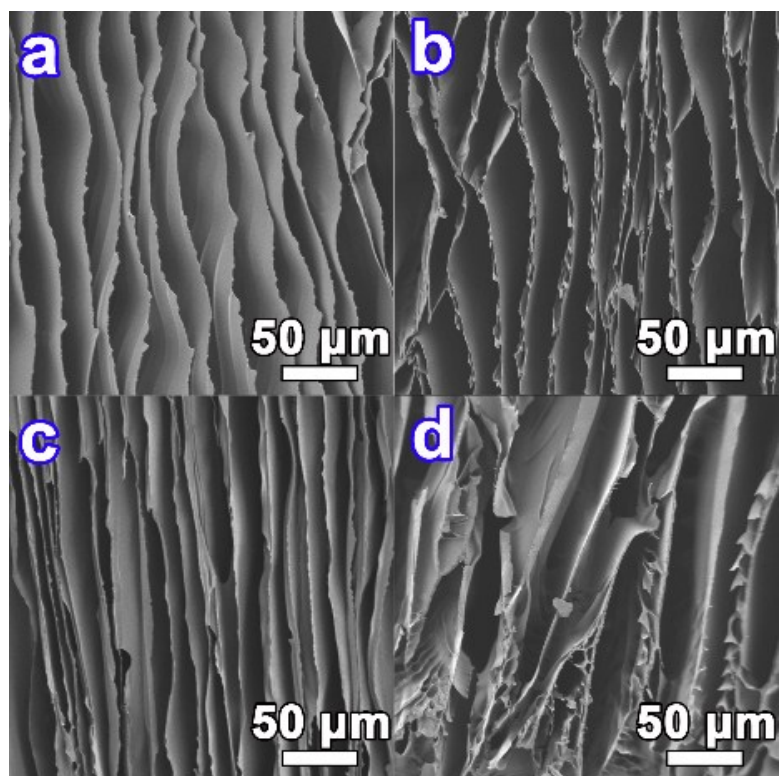
Fig. S3 SEM images of laminated CS arrays after freeze drying from aqueous solutions of (a-d) 3, 4, 5, 6 wt% CS, respectively.
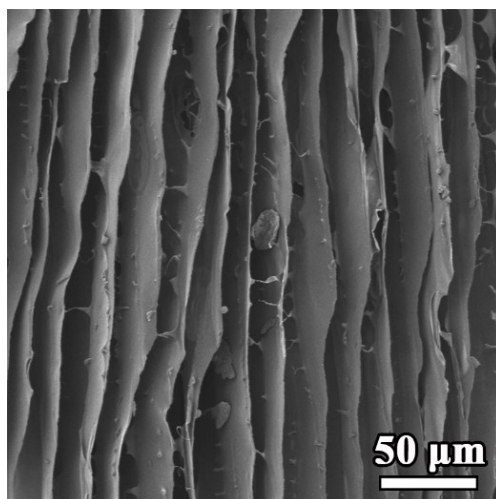
Fig. S4 SEM image of laminated NC array.
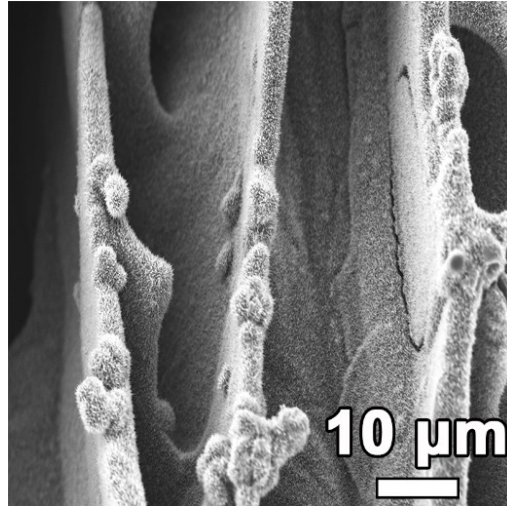
Fig. S5 Magnified SEM image of laminated MONPMs/NC arrays in Fig. 2a.
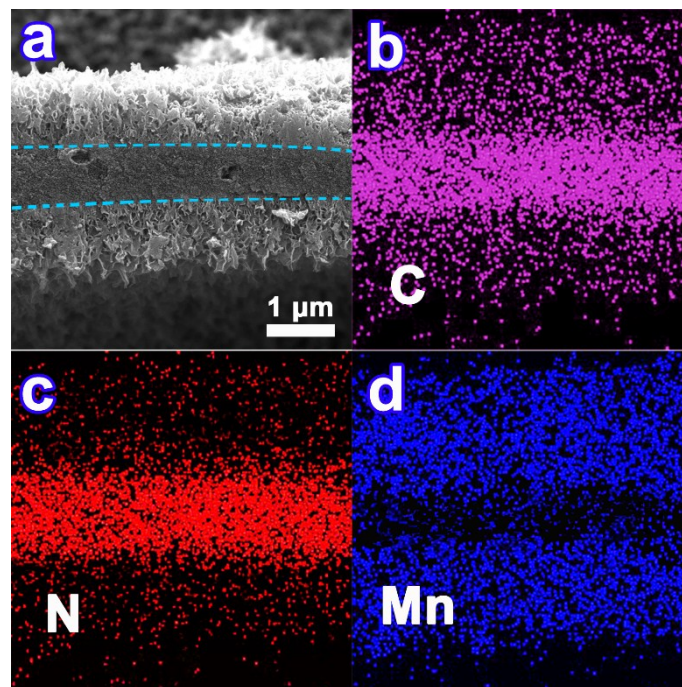
Fig. S6 (a) SEM image and (b, c and d) C, N, and Mn mapping images of a laminate of MONPMs/NC, where two layers of MONPMs grow separately on both surfaces of a laminate of NC. The dotted lines illustrate the interface between NC and MONPMs.
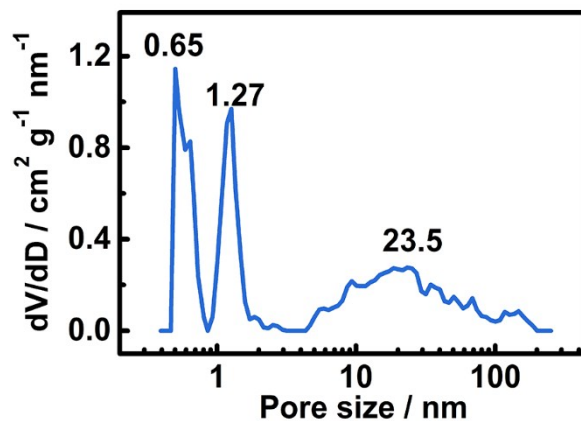
Fig. S7 The pore size distribution of MONPMs/NC.
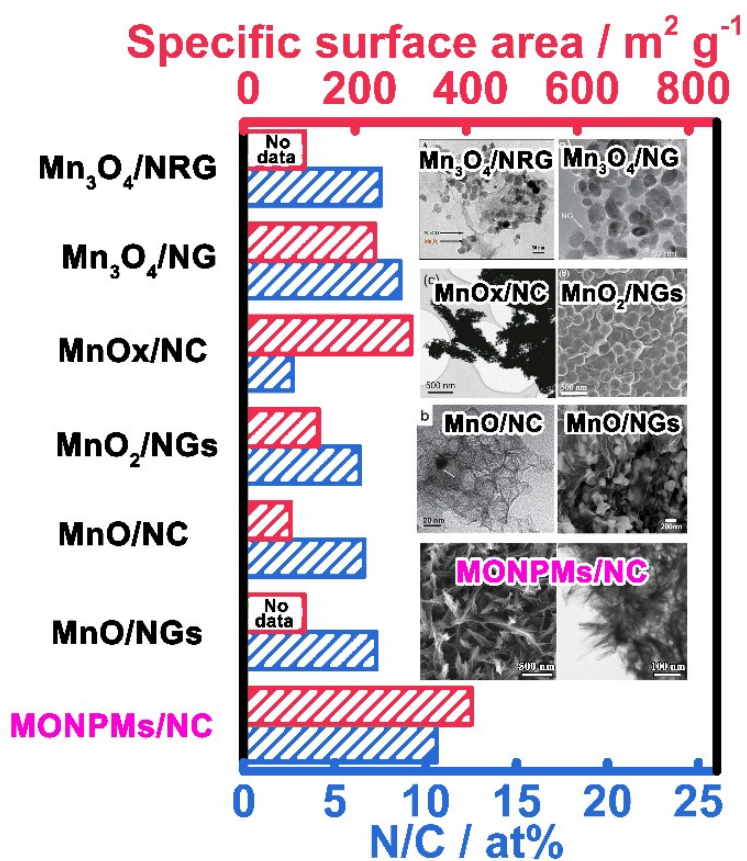
Fig. S8 Comparison of (inset) morphology, N content and specific surface area of MONPMs/NC with reported MnOx/N doped carbon[3-8]. The insets are adapted from references with copyright from Elsevier, Wiley-VCH, American Chemical Society and The Royal Society of Chemistry, respectively.
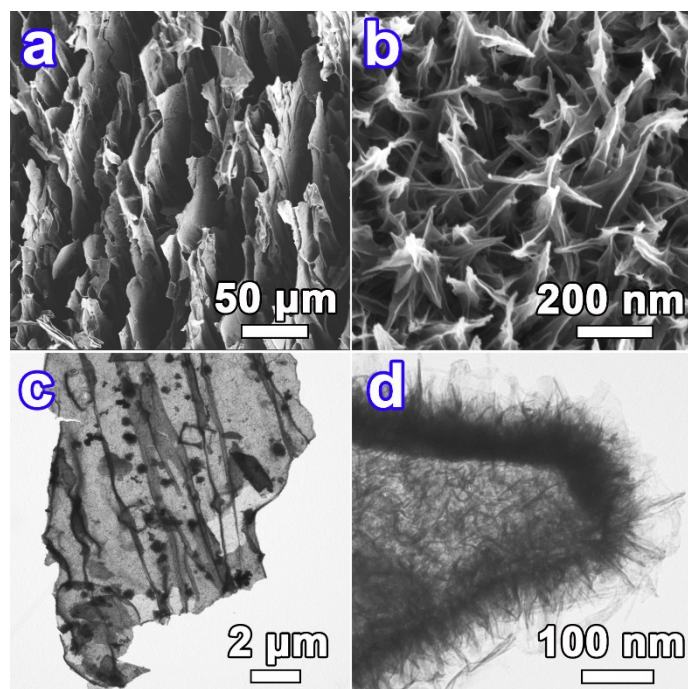
Fig. S9 (a) SEM image and (b) magnified SEM image, (c) TEM image and (d) magnified TEM image of MONPMs.
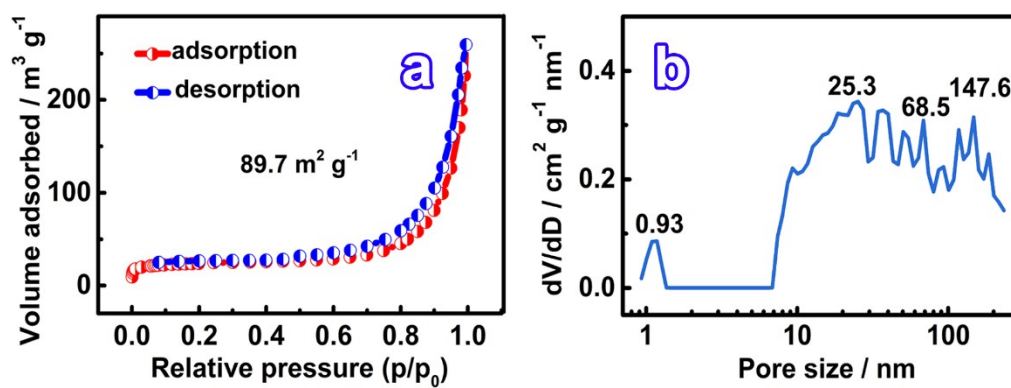
Fig. S10 (a) N_2 adsorption-desorption isotherms at -196 ^{o}C, (b) pore size distribution of MONPMs.
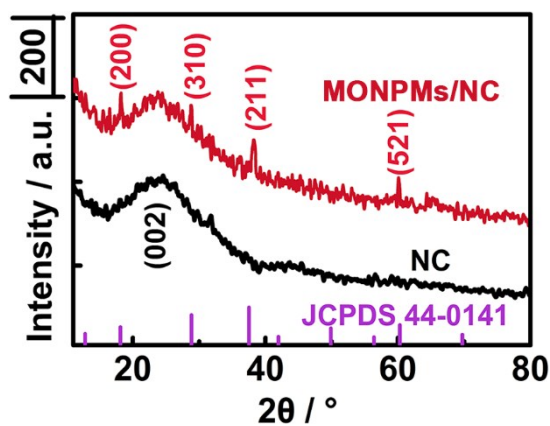
Fig. S11 XRD patterns of NC, MONPMs/NC and α-MnO$_2$ (JCPDS 44-0141).
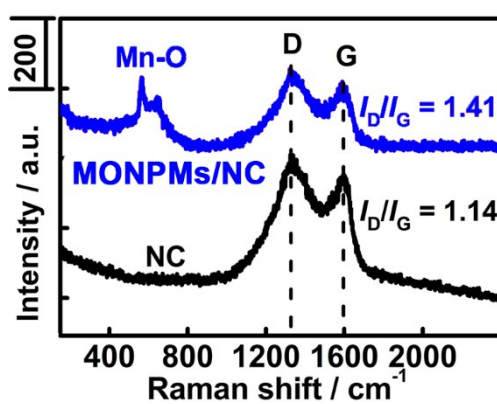
Fig. S12 Raman spectra of NC and MONPMs/NC
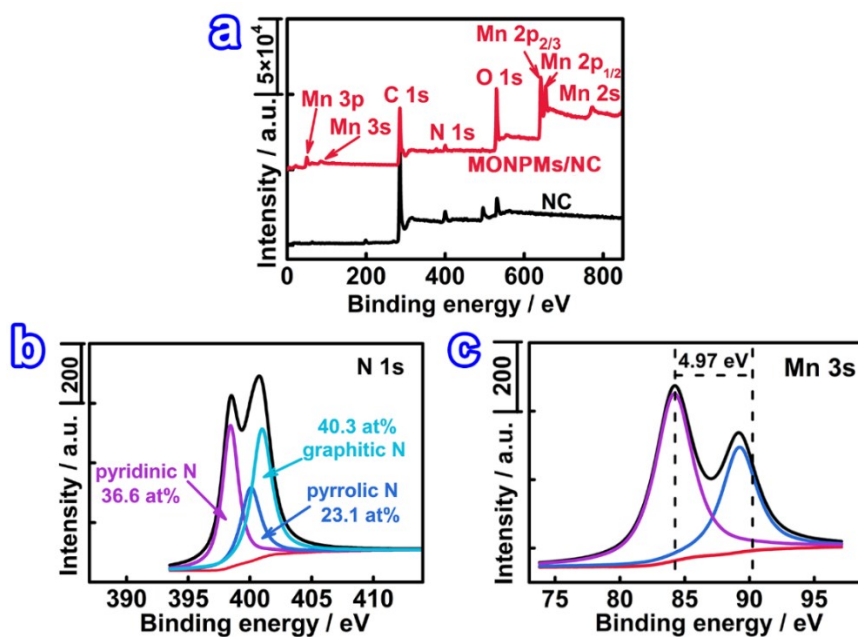
Fig. S13. (a) XPS spectra of NC and MONPMs/NC. (b) N 1s and (c) Mn 2p XPS spectra of MONPMs/NC.
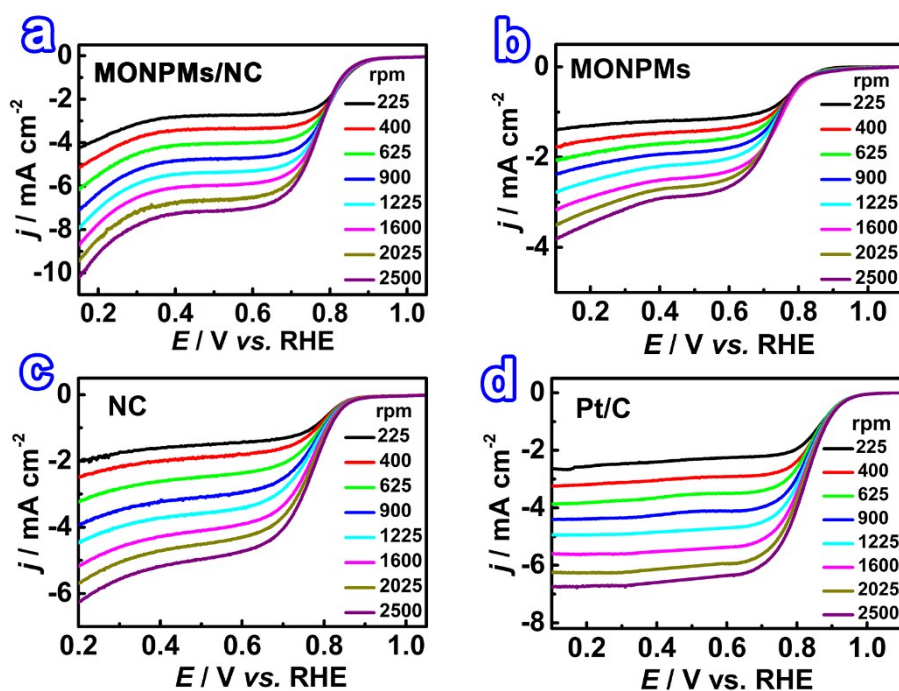
Fig. S14. LSV curves of (a) MONPMs, (b) NC (c) MONPMs/NC and (d) commercial Pt/C for the ORR in an O_2-saturated aqueous solution of 0.1 M KOH at the scan rate of 5 mV s^{-1} with different rotating speeds.
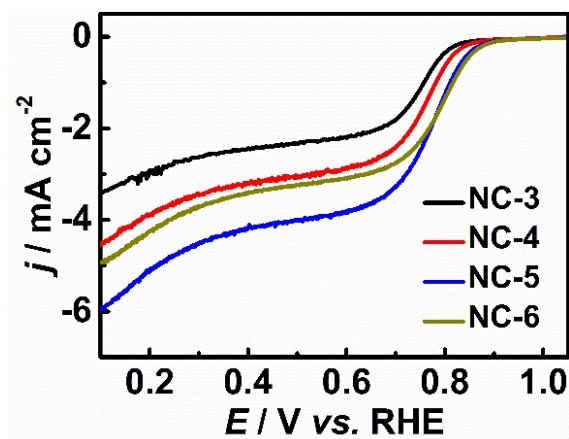
Fig. S15 LSV curves of NCs for ORR. NC-3, 4, 5, 6 represent NC derived from CS with concentration of 3, 4, 5, 6 wt%, respectively.
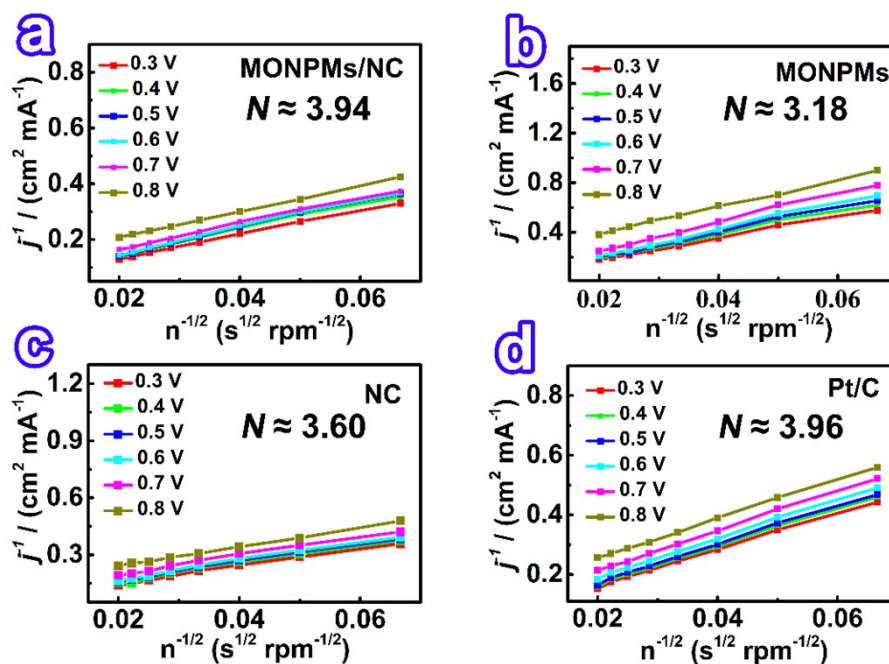
Fig. S16. K–L plots and the average electron transfer number (*N*) of (a) MONPMs/NC, (b) MONPMs, (c) NC and (d) Pt/C.
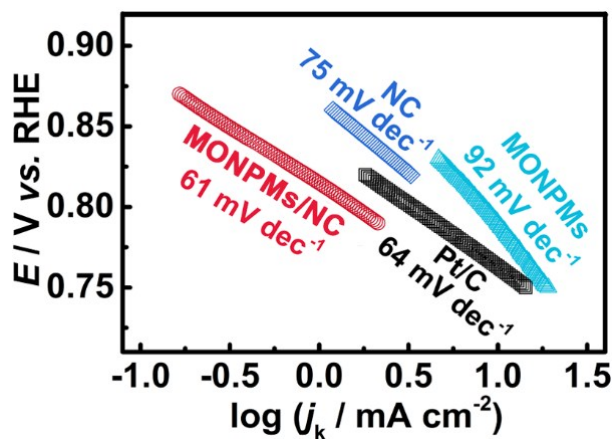
Fig. S17 Tafel plots of MONPMs, NC, MONPMs/NC and commercial Pt/C catalysts.
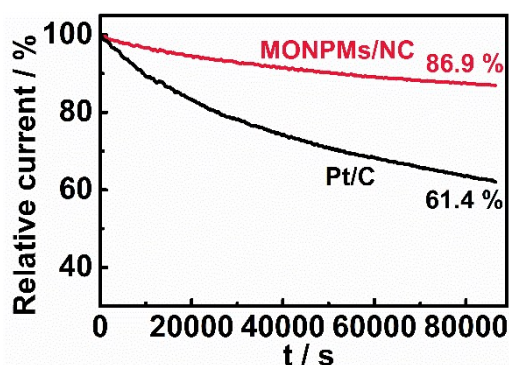
Fig. S18 Chronoamperometric responses of MONPMs/NC and Pt/C catalysts for 86400 s.
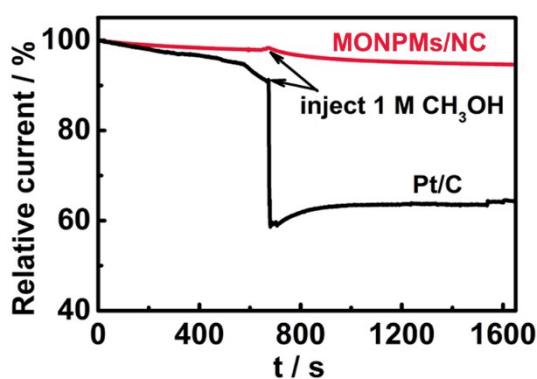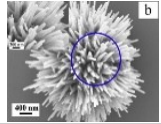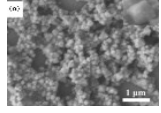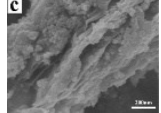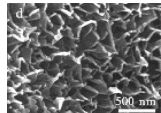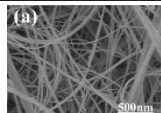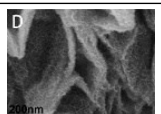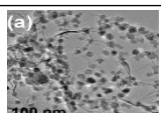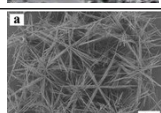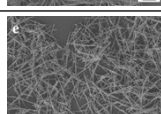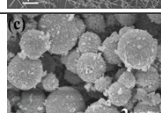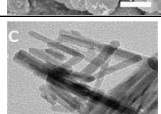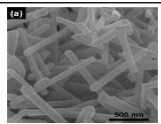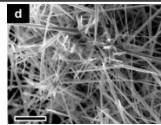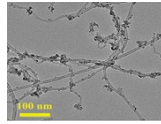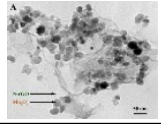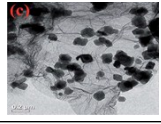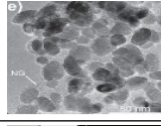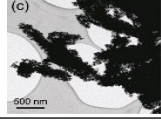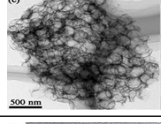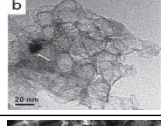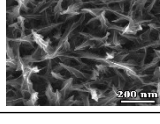
Fig. S19 Chronoamperometric responses of MONPMs/NC and commercial Pt/C catalysts in an O_2-saturated aqueous solution of 0.1 M KOH to injection of 1 M methanol.
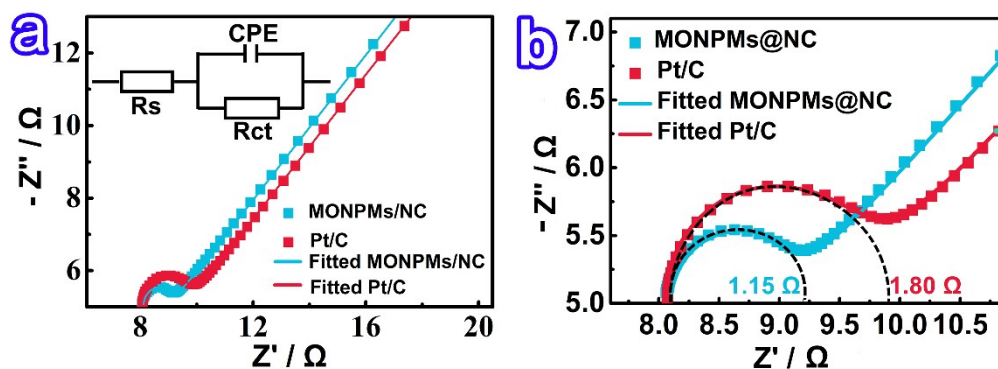
Fig. S20 (a) Nyquist plots and (b) high-frequency range Nyquist plots of MONPMs/NC and Pt/C from EIS measurements in O_2-saturated 0.1 M KOH solution. The inset in Fig. S20a is an equivalent circuit where Rs is the series resistance, Rct is the charge transfer resistance and CPE is the constant-phase element normally introduced to replace the double layer capacitance to better describe the real capacitance of the electrode.

Table S1 Comparisons of morphology, specific surface area and catalytic data of MONPMs/NC with reported MnO_x, heteroatoms doped MnO_x and MnO_x/carbon catalysts for ORR.

	Morphology	Specific surface areas ($m^2 g^{-1}$)	Onset potential (V)	N	$E_{1/2}$ (V)	Durability	Ref.
α-MnO_2		27.7	0.85	3.8	0.73	36000 s 85 %	J. Power Sources 2017, 362, 332.
MnO/rGO		--	0.81	3.95	0.62	20000 s 62 %	J. Mater. Sci. 2017, 52, 6656.
Mn_3O_4/rGO		89	0.86	3.96	0.76	20000 s 88.5 %	J. Colloid Interface Sci. 2017, 488, 251.
α-MnO_2		78.3	0.85	4.18	0.72	36000 s 88.09%	CrystEngComm 2016, 18, 6895.
Co-MONSs/MC		--	0.97	3.64	0.68	43200 s 86.9 %	Appl. Mater. Today 2016, 3, 63.
α-MnO_2		57.81	0.94	3.90	0.72	61200 s 80 %	Inorg. Chem. Front. 2016, 3, 928.
MnO_2/rGO		183	0.83	3.85	0.69		Int. J. Hydrogen Energy 2016, 41, 5260.
Co_3O_4-Mn_3O_4/GO		--	0.87	3.90	0.78	7000 s 94.61%	Nano Energy 2016, 27, 185.
α-MnO_2		14.9	0.84	3.81	0.72	36000 s 93.3%	J. Mater. Chem. A 2016, 4, 16462.
α-MnO_2		24.5	0.93	3.8	0.75		J. Power Sources 2015, 280, 526.
MnO_x		44.57	0.93	3.9	0.73	43200 s 93.0%	Chem. Commun. 2015, 51, 11599.
α-MnO_2		112	0.89	3.7	0.79		J. Am. Chem. Soc. 2014, 136, 11452.

Catalyst						Stability	Reference
C-α-MnO$_2$ NWs		73.6	0.88	3.84	0.75		ACS Appl. Mater. Interfaces 2018, 10, 2040.
Ni-α-MnO$_2$		-	0.89	3.66	0.70		J. Phys. Chem. C 2017, 121, 2789.
CMO@CNTs		203.6	0.97	3.70	0.85		Inorg. Chem. Front. 2017, 4, 1628.
N-rGO-Mn$_3$O$_4$		--	0.93	3.75	0.73	10000 s 86 %	ACS Appl. Mater. Interfaces 2014, 6, 2692.
MnO/NG		--	0.89	3.7	0.77	10 000 cycles 80 %	RSC Adv. 2016, 6, 95590.
NENG		85	0.87	3.81		36000 s 79 %	Adv. Funct. Mater. 2014, 24, 2072.
MnO$_x$/NC		135	0.95		0.80	36000 s 80 %	Green Chem. 2017, 19, 2793.
MnO$_2$/N-HGSs		302	0.94	3.85	0.84	12 h 85 %	ACS Appl. Mater. Interfaces 2016, 8, 35264.
MnO-m-N-C		236	0.92	3.84	0.81	10000 s 97 %	Adv. Funct. Mater. 2012, 22, 4584.
MONPMs/NC		409.7	0.98	3.90	0.81	86400 s 86.9 %	This work

N: electron transfer number; $E_{1/2}$: halfwave potential;

rGO: reduced graphene oxide; Co-MONSs/MC: Co doped MnO$_2$ nanosheets (MONSs) on the macroporous carbon

(MC); MnO$_x$/S-GC: MnO$_x$/S doped graphitized carbon; C-α-MnO$_2$ NWs: carbon-coated α-MnO$_2$ nanowires;

CMO@CNTs: Co–Mn–O supported on carbon nanotubes;

NENG: Mn$_3$O$_4$ quasi-nanoellipsoids on nitrogen-doped graphene;

NG: N-doped graphene; m-N-C: mesoporous N-doped carbon.

References and notes

1. L. B. Mao, H. L. Gao, H. B. Yao, L. Liu, H. Cölfen, G. Liu, S. M. Chen, S. K. Li, Y. X. Yan, Y. Y. Liu and S. H. Yu, *Science*, 2016, **354**, 107-110.

2. H. L. Gao, Y. B. Zhu, L. B. Mao, F. C. Wang, X. S. Luo, Y. Y. Liu, Y. Lu, Z. Pan, J. Ge, W. Shen, Y. R. Zheng, L. Xu, L. J. Wang, W. H. Xu, H. A. Wu and S. H. Yu, *Nat. Commun.*, 2016, **7**, 12920.

3. S. Bag, K. Roy, C. S. Gopinath and C. R. Raj, *ACS Appl. Mater. Interfaces*, 2014, **6**, 2692-2699.

4. J. Duan, S. Chen, S. Dai and S. Qiao, *Adv. Funct. Mater.*, 2014, **24**, 2072-2078.

5. J. Pandey, B. Hua, W. Ng, Y. Yang, K. van der Veen, J. Chen, N. J. Geels, J. Luo, G. Rothenberg and N. Yan, *Green Chem.*, 2017, **19**, 2793-2797.

6. Q. Yu, J. Xu, C. Wu, J. Zhang and L. Guan, *ACS Appl. Mater. Interfaces*, 2016, **8**, 35264-35269.

7. Y. Tan, C. Xu, G. Chen, X. Fang, N. Zheng and Q. Xie, *Adv. Funct. Mater.*, 2012, **22**, 4584-4591.

8. K. Zhang, P. Han, L. Gu, L. Zhang, Z. Liu, Q. Kong, C. Zhang, S. Dong, Z. Zhang, J. Yao, H. Xu, G. Cui and L. Chen, *ACS Appl. Mater. Interfaces*, 2012, **4**, 658-664.